Implementation-Oriented Model for Centralized Data-Fusion Cooperative Spectrum Sensing

Dayan Adionel Guimarães and Rausley Adriano Amaral de Souza, *Member, IEEE*

***Abstract*—We propose a new model for a cognitive radio in the scenario of centralized data-fusion cooperative spectrum sensing. The model is grounded on a direct-conversion receiver architecture and was applied to four detection methods: the eigenvalue-based generalized likelihood ratio test, the maximum-minimum eigenvalue detection, the maximum eigenvalue detection and the energy detection. It is shown that the sensing performance under the conventional model typically adopted in the above scenario is overestimated when compared with the proposed one, which suggests that our model better suits for the spectrum sensing design and its performance assessment.**

***Index Terms*—Cognitive radio, cooperative spectrum sensing.**

I. Introduction

SPECTRUM sensing is the task of detecting spectral holes in bands licensed to primary wireless networks, for opportunistic use by secondary cognitive radios (CR). This sensing can be independently made by each CR, but cooperative sensing [1], [2] has been considered the solution for receiver uncertainty, multipath fading and shadowing. Among the spectrum sensing techniques, eigenvalue-based ones are receiving a lot of attention [3], [4], mainly because no prior information about the transmitted signal is necessary. In some techniques, the knowledge of the noise power is not needed as well [4]. Conventionally, the multiple-input, multiple-output (MIMO) discrete time channel model has been indistinctively adopted for modeling the received samples for single-receiver, multi-antenna and for multiple-receiver, single-antenna sensing devices in data-fusion centralized cooperative spectrum sensing. However, without an appropriate modification, this model is not well suited to the case of single-antenna multiple receivers. This modification is needed because the conventional model assumes that samples collected by each CR are forwarded to the fusion center (FC) as if no signal processing task is performed at the CRs. To the best of our knowledge, no exception to this assumption has been considered so far.

In this letter we propose a new implementation-oriented model in which typical signal processing tasks of a direct-conversion CR receiver are taken into account. In order to compare our results with those reported in the literature, we investigate the performances of four well-known sensing schemes [4] under the conventional and the new model, namely: the eigenvalue-based generalized likelihood ratio test (GLRT), the maximum-minimum eigenvalue detection (MMED), also known as eigenvalue ratio detection (ERD), the maximum eigenvalue detection (MED), also known as Roy's largest root test (RLRT), and the energy detection (ED).

Manuscript received July 25, 2012. The associate editor coordinating the review of this letter and approving it for publication was W. Zhang.

The authors are with the National Institute of Telecommunications (Inatel), PO Box 05, 37540-000 Santa Rita do Sapucaí - MG - Brazil (e-mail: {dayan, rausley}@inatel.br).

Digital Object Identifier 10.1109/LCOMM.2012.12.121614

II. Conventional Model

Let a discrete-time MIMO model in which there are m single-antenna cognitive receivers or m antennas in a cognitive receiver, each one collecting n samples of the received signal from p primary transmitters during the sensing period. These samples are arranged in a matrix $\mathbf{Y} \in \mathbb{C}^{m\times n}$ and the samples from the p transmitters are arranged in a matrix $\mathbf{X} \in \mathbb{C}^{p\times n}$. Let $\mathbf{H} \in \mathbb{C}^{m\times p}$ be the channel matrix with elements $\{h_{ij}\}$, $i = 1, 2, \ldots, m$ and $j = 1, 2, \ldots, p$, representing the channel gains between the j-th primary transmitter and the i-th sensor (antenna or receiver). Finally, let $\mathbf{V} \in \mathbb{C}^{m\times n}$ be the matrix containing noise samples that corrupt the received signals. The matrix of received samples is then $\mathbf{Y} = \mathbf{HX} + \mathbf{V}$. In eigenvalue-based sensing, spectral holes are detected using test statistics based on the eigenvalues of the sample covariance matrix of the received signal matrix $\mathbf{Y}$. If a multi-antenna device is used for non-cooperative sensing, or even for centralized cooperative sensing with data-fusion, the sample covariance matrix will be $\mathbf{R} = \mathbf{YY}^{\dagger}/n$, where $\dagger$ means complex conjugate and transpose. When centralized cooperative sensing with single-antenna CRs is considered, the matrix $\mathbf{Y}$ is the one that is assumed to be available at the FC as if no signal processing is needed before each row of $\mathbf{Y}$ is sent to the FC.

III. Implementation-Oriented Model

The diagram shown in Fig. 1 is a possible reference for constructing a more realistic model. It combines a direct conversion receiver (DCR) front-end with spectrum-sensing-directed functions. The analog RF front-end comprises a wide-band antenna, a wideband band-pass filter (BPF), a low-noise amplifier (LNA) and quadrature local oscillators (LO) and mixers responsible for direct conversion of the desired channel to in-phase and quadrature (I&Q) baseband signals. DCRs, though attractive from the perspective of circuit integration, suffer from drawbacks like I&Q imbalance, flicker noise and DC-offset [5]. Among these, DC-offset is the most damaging and, without compensation, can easily saturate subsequent amplification stages [6]. It is a DC signal appearing at the mixer output, primarily due to LO self-mixing processes and in-band interfering signals, and it is composed of a static and a dynamic part. By adopting careful circuit design and modern DC-offset compensation algorithms, the static part can be almost completely eliminated, whereas some residual dynamic DC-offset will always remain [7]. The summation block following the mixer in Fig. 1 accounts for this residual dynamic DC-offset.

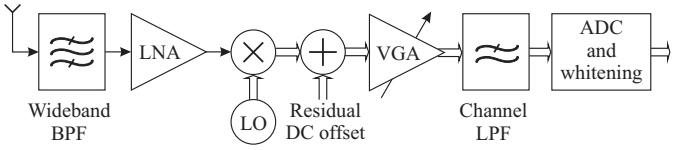

Fig. 1. Direct conversion cognitive radio receiver.

The resultant I&Q signals then go through a variable gain amplifier (VGA), which is part of an automatic gain control (AGC) mechanism responsible for maintaining the signal within the dynamic range of the analog-to-digital converters (ADC) in the I&Q signal paths. I&Q low-pass filters (LPF) select the desired bandwidth to be sampled. The noise whitening process takes place to guarantee that noise samples are kept uncorrelated when $\mathbf{Y}$ is built at the FC.

IV. Simulation Description

The simulation setup under the proposed model has been built to adhere to the overall centralized data-fusion cooperative spectrum sensing scenario and to the spectrum-sensing-directed receiver architecture depicted in Fig. 1. To simulate a noise-like transmitted signal with controllable time correlation at the receiver side, $\mathbf{X}$ is formed by filtering independent and identically distributed (iid) complex Gaussian samples with a length-L moving average (MA) filter with no quantization (using floating-point computations). This type of filter has been chosen for simplicity reasons; any other low-pass filter could be adopted as well. The Gaussian distribution for the entries of $\mathbf{X}$ has been adopted because it accurately models several modulated signals. The elements in $\mathbf{H}$ are zero mean iid complex Gaussian variables that simulate a flat Rayleigh fading channel between each transmitter and sensor, assumed to be constant during a sensing period and independent from one period to another. To simulate the filtering effects at the CRs, the entries in $\mathbf{V}$ are MA-filtered complex Gaussian variables that represent the colored additive thermal noise. The memory elements in the structure of the above MA filtering processes are assumed to have zero initial value before the first valid sample is applied to their inputs. As a result, the first $(L-1)$ samples from the MA filtering, out of $(n+L-1)$, are discarded before subsequent operations. Filtered samples has been normalized to guarantee the desired signal-to-noise ratio (SNR), in dB. Specifically, $\mathbf{X} \leftarrow \mathbf{X}/\sqrt{P_X}$ for unitary received primary signal power and $\mathbf{V} \leftarrow (\mathbf{V}/\sqrt{P_V})\sqrt{10^{-\mathrm{SNR}/10}}$ for an SNR-dependent thermal noise power, where P_X and P_V are the time-series average powers in $\mathbf{X}$ and $\mathbf{V}$ before normalization, respectively. Matrix $\mathbf{H}$ is also normalized so that $(1/mp)\|\mathbf{H}\|_F^2 = (1/mp)\mathrm{tr}(\mathbf{H}^\dagger\mathbf{H}) = 1$, where $\|\cdot\|_F$ and $\mathrm{tr}(\cdot)$ are the Frobenius norm and the trace of the underlying matrix, respectively. The effect of the LNA and the AGC at the i-th CR, $i = 1, 2, \ldots, m$ is produced by the gain

$$g_i = \frac{f_{\mathrm{od}} D\sqrt{2}}{6\sqrt{\frac{1}{n}\mathbf{y}_i^\dagger \mathbf{y}_i}} = \frac{f_{\mathrm{od}} D\sqrt{2n}}{6\|\mathbf{y}_i\|_2}, \qquad (1)$$

where $\mathbf{y}_i$ is the vector of n samples collected by the i-th CR and $\|\mathbf{y}_i\|_2$ is the Euclidian norm of $\mathbf{y}_i$. The reasoning behind proposing these gains is explained as follows: The combined gains of the LNA and the AGC are those that maintain the signal amplitude at the inputs of the I&Q ADCs within their dynamic ranges D. By dividing the sample values by the square root of $\mathbf{y}_i^\dagger \mathbf{y}_i/n$, which is the average power of $\mathbf{y}_i$, one obtains samples with unitary average power. Since $\mathbf{X}$ is Gaussian, $\{\mathbf{y}_i\}$ have Gaussian distributed sample values, conditioned on the corresponding channel gain. If σ^2 is the variance of these (complex) samples after the effect of the LNA/AGC, to guarantee that six standard deviations (practically the whole signal excursion or 99.73% of the sample values) of the I&Q signals will be within $[-D/2, D/2]$, we shall have $6\sqrt{\sigma^2/2} = D$, which means that the signal power at the output of the AGC will be $\sigma^2 = 2D^2/36$. This justifies the factor $D\sqrt{2}/6$ in (1). The overdrive factor $f_{\mathrm{od}} \geq 1$ is included in (1) to simulate different levels of signal clipping caused by the ADCs. The clipping acts in a sample value s according to $s \leftarrow \mathrm{sign}(s)\min(|s|, D/2)$, where D is the dynamic range of the ADCs. If $f_{\mathrm{od}} = 1$, the resultant gain will guarantee that six standard deviations of I&Q signals will be within $[-D/2, D/2]$. Practical AGC circuits do not exhibit perfect adjusting precision as in (1), since they work stepwise. However, it is a reasonable assumption to consider modern numeric-controllable variable attenuators and digitally controlled VGA working together a digital signal process which normalizes the ADCs output signals according to their estimated average powers, so that an overall fine adjusting precision is achieved. Following the arguments in [8], the DC-offset is assumed to be a complex-valued Gaussian random variable with zero mean, constant over one sensing period and independent from one period to another. This is translated into the matrix $\mathbf{D} \in \mathbb{C}^{m\times n}$ that will be considered when forming the received signal matrix, according to $\mathbf{Y} = \mathbf{HX} + \mathbf{V} + \mathbf{D}$. The elements in $\mathbf{D}$ are column-wise equal to one another within a given sensing period, though different in different sensing periods, and are zero mean row-wise iid complex Gaussian variables to represent independent DC-offsets among CRs. The effect of the ADC on the sample values that will be forwarded to the FC is produced by a quantizer with configurable number N_{q} of quantization levels. The whitening filter matrix that multiplies the MA-filtered, amplified and perhaps clipped versions of $\{\mathbf{y}_i\}$ is computed according to $\mathbf{W} = \mathbf{UC}^{-1}$, where $\mathbf{U}$ is the orthogonal matrix from $\mathbf{Q} = \mathbf{U\Sigma K}^T$, the singular-value decomposition (SVD) of the matrix $\mathbf{Q}$ whose elements are $Q_{ij} = a_{|i-j|}$, with $\{a_k\}$ representing the discrete autocorrelation function of the MA filter impulse response, i.e. $a_k = (1 - k/L)$, for $k \leq L$, and $a_k = 0$ otherwise, for $i, j, k = 0, 1, \ldots, (n-1)$. Matrix $\mathbf{C}$ is the lower triangular matrix from the Cholesky decomposition of $\mathbf{Q}$. Notice that this is a signal-independent whitening process that can be easily implemented in practice, since matrix $\mathbf{W}$ is pre-computed at the system design phase.

From the modified received matrix $\mathbf{Y} = \mathbf{HX} + \mathbf{V} + \mathbf{D}$, matrix $\mathbf{R} = \mathbf{YY}^\dagger/n$ is then formed at the FC, from which the eigenvalues $\{\lambda_1 \geq \lambda_2 \geq \cdots \lambda_m\}$ are estimated. The test statistics for the GLRT, MMED, MED and ED are then computed according to [4]

$$T_{\mathrm{GLRT}} = \frac{\lambda_1}{\frac{1}{m}\mathrm{tr}(\mathbf{R})} = \frac{\lambda_1}{\frac{1}{m}\sum_{i=1}^{m}\lambda_i} \qquad (2)$$

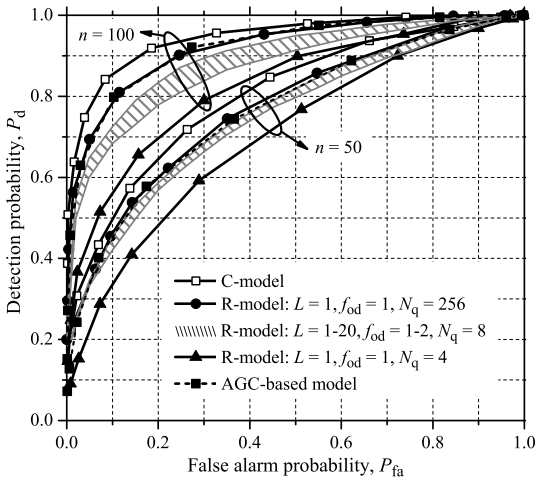

Fig. 2. ROC for the GLRT under the conventional and the proposed models.

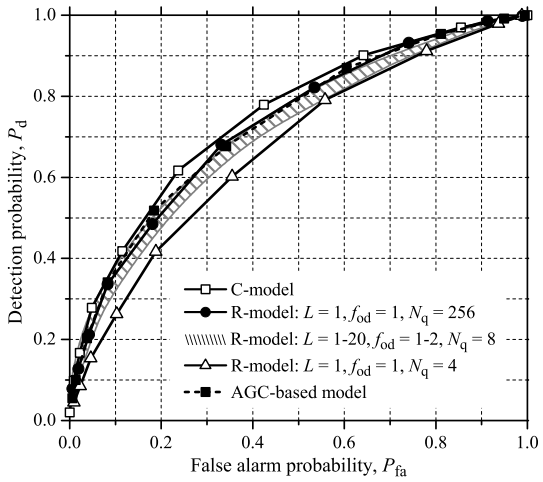

Fig. 3. ROC for the MMED under the conventional and the proposed models.

$$T_{\text{MMED}} = \lambda_1/\lambda_m \tag{3}$$

$$T_{\text{MED}} = \lambda_1/\sigma^2 \tag{4}$$

$$T_{\text{ED}} = \frac{\|\mathbf{Y}\|_F^2}{mn\sigma^2} = \frac{\sum_{i=1}^{m}\lambda_i}{m\sigma^2}, \tag{5}$$

where σ^2 is the thermal noise power, assumed to be known and the same in each sensor input. The test statistic for a specific detection technique is compared with a threshold computed from the desired probability of false alarm (P_{fa}), and a final decision upon the occupancy of the sensed channel is reached.

V. Numerical Results

The receiver operating characteristic (ROC) curves shown hereafter were obtained with a minimum of $5,000$ runs of Monte Carlo simulations. First we consider that the DC-offset in the system model shown in Fig. 1 is zero. Non-zero DC-offset is considered subsequently.

A. Zero DC-offset

Figs. 2, 3 and 4 show ROC curves relating P_{fa} and the probability of detection (P_{d}) for the investigated detection techniques, for $p = 1$, $m = 6$, SNR $= -10$ dB, and variable L, N_{q} and f_{od}. The shaded areas in these figures represent positions of ROC curves for $N_{\text{q}} = 8$, and for f_{od} and L ranging from 1 to 2, and 1 to 20, respectively. These shaded areas are meant to reflect parameter variations within empirical limits of practical significance for the model based on Fig. 1 (R-model). Since the influence of increasing the number n of collected samples per CR is, as expected, a performance improvement considering fixed the remaining system parameters, only Fig. 2 considers both $n = 50$ and $n = 100$. To avoid polluting unnecessarily the graphs, only $n = 50$ is considered in Figs. 3 and 4. The results labeled "AGC-based model" will be discussed in the last section of the paper.

It can be seen from Figs. 2, 3 and 4 that the performances under the R-model are significantly degraded for $N_{\text{q}} = 4$, and that they change slightly from $N_{\text{q}} = 8$ to $N_{\text{q}} = 256$. It can also be seen that the performances under the conventional model (C-model), whose results are in close agreement with those in [4], are overestimated if compared with the proposed model, mainly for MED and ED. Particularly in the case of ED, the performance does not improve even for n as large as 500. This is an indication that, if a real receiver is used in a data-fusion centralized cooperative sensing, and if the decision statistic needs the noise variance information, the effect of the AGC loop must be taken into account not only in the noise variance estimate, but also in the definition of the test statistic itself. The analysis of the influence of the AGC in the noise variance estimate and in the test statistic is an opportunity for further contributions related to the model proposed here.

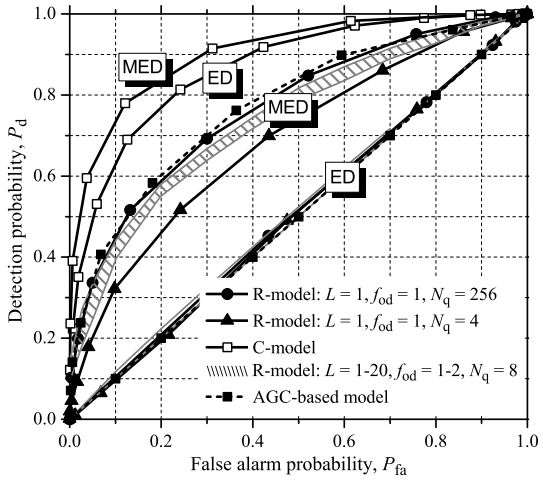

Fig. 4. ROC for MED and ED under the conventional and proposed models.

B. Non-Zero DC-offset

Now we present numerical results considering that a residual dynamic DC-offset is present. The SDCR (signal-to-DC-offset power ratio) and the impulse response length of the receive filter, L, are the parameters varied to assess system performance. Other systems parameters are $m = 6$, $n = 50$, $p = 1$, SNR $= -10$ dB, $f_{\text{od}} = 1.2$ and $N_{\text{q}} = 8$. Due to the lack of space, we present in Fig. 5 only results for the GLRT technique. We attest, however, that very similar behaviors were observed for MMED and MED, and that all conclusions drawn

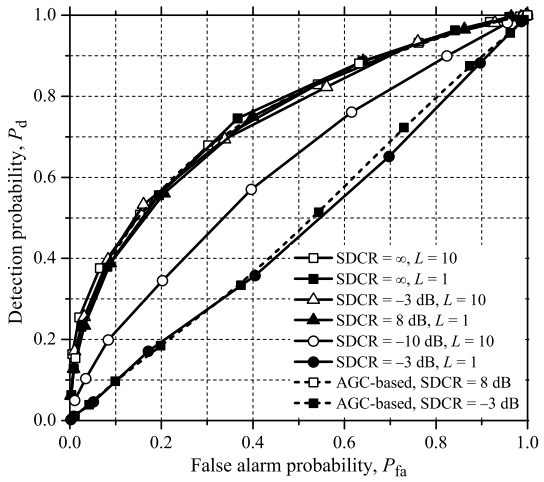

Fig. 5. ROC for the GLRT for non-zero residual dynamic DC-offset.

from the GLRT also apply to them. As before, ED does not work at all under R-model.

The first important observation from Fig. 5 is that system performance becomes less sensitive to the DC-offset for larger values of L. This is justified by the fact that the whitening process, which takes place if $L > 1$, also decorrelates the highly correlated DC-offset values from sample to sample. The curves that are grouped together for finite SDCRs are for minimum SDCR values that keep them grouped. This means that, for $L = 1$, the sensing performance is practically insensitive to a residual DC-offset for which SDCR ≥ 8 dB. If $L = 10$, system robustness against DC-offset increases, and it works for SDCR ≥ -3 dB as if no DC-offset existed. When the received signal is not too week and the RF and DC-offset compensation circuitry are properly designed, the residual SDCR can be on the order of 15 to 30 dB [9]. In such cases, one can disregard the effect of the residual DC-offset on the system performance if the model depicted in Fig. 1 is adopted.

VI. AGC-BASED MODEL

From the previous results, one can infer that that the AGC has caused most of the influence in the detection performance. This is confirmed by observing the dashed curves right above the shaded areas in Figs. 2, 3 and 4, and also in Fig. 5, which were obtained using what we are calling an AGC-based model. In this model, the received signal covariance matrix becomes

$$\mathbf{R}' = \mathbf{Y}'\mathbf{Y}'^{\dagger}/n = \mathbf{G}\mathbf{Y}(\mathbf{G}\mathbf{Y})^{\dagger}/n = \mathbf{G}\mathbf{R}\mathbf{G}, \qquad (6)$$

where $\mathbf{G}$ is a diagonal AGC gain matrix whose entries are obtained from (1), omitting constants that do not influence system performance if no additional signal processing are taken into consideration besides AGC, i.e.

$$G_{ii} = (\mathbf{y}_i^{\dagger}\mathbf{y}_i)^{-0.5} = \|\mathbf{y}_i\|_2^{-1}. \qquad (7)$$

From Fig. 5 it can be noticed that this AGC-based model is also valid in the presence of a residual dynamic DC-offset, as long as SDCR ≥ 8 dB. This model is the proposed mathematical counterpart of the circuit-based model constructed from the diagram in Fig. 1. Analytical investigations under this model also represent an opportunity for further contributions.

VII. CONCLUSIONS AND FINAL REMARKS

An implementation-oriented model was proposed for centralized data-fusion cooperative spectrum sensing. A mathematical AGC-based version of this model was also suggested. Simulation results showed that the detection performance under the conventional model can be overestimated when compared with the proposed one. In our model, the AGC will affect the noise level that corrupts the received samples, from where it can be concluded that ED and eigenvalue-based techniques that demand the knowledge of the noise variance, like the RLRT, are feasible only if this AGC effect is taken into account in the noise variance estimated value, as well as in the decision statistic formulae. The degraded performances of MED and ED in Fig. 4 support this statement. From the influence of the quantization levels, we can conclude that 3 bits per sample are enough for the transmission of the sample values to the FC, a result that is useful for determining the necessary bandwidth and traffic over the reporting channel. One last conclusion is that, for properly designed RF and DC-offset compensation circuitry, the sensing performance under the implementation-oriented model can be practically insensitive to typical residual dynamic DC-offsets. We reiterate that this is valid for all detection techniques considered here, though results were presented only for the GLRT.

REFERENCES

[1] W. C. Headley, V. G. Chavali, and C. R. C. M. da Silva, "Exploiting radio correlation and reliability information in collaborative spectrum sensing," *IEEE Commun. Lett.*, vol. 15, no. 8, pp. 825–827, Aug. 2011.

[2] A. Singh, M. R. Bhatnagar, and R. K. Mallik, "Cooperative spectrum sensing in multiple antenna based cognitive radio network using an improved energy detector," *IEEE Commun. Lett.*, vol. 16, no. 1, pp. 64–67, Jan. 2012.

[3] A. Kortun, T. Ratnarajah, M. Sellathurai, C. Zhong, and C. B. Papadias, "On the performance of eigenvalue-based cooperative spectrum sensing for cognitive radio," *IEEE J. Sel. Topics Signal Process.*, vol. 5, no. 1, pp. 49–55, Feb. 2011.

[4] B. Nadler, F. Penna, and R. Garello, "Performance of eigenvalue-based signal detectors with known and unknown noise level," in *Proc. 2011 IEEE Int. Conf. on Commun.*, pp. 1–5.

[5] B. Razavi, "Design considerations for direct-conversion receivers," *IEEE Trans. Circuits Syst. II*, vol. 44, no. 6, pp. 428–435, June 1997.

[6] R. Svitek and S. Raman, "DC offsets in direct-conversion receivers: characterization and implications," *IEEE Microw. Mag.*, vol. 6, no. 3, pp. 76–86, Sep. 2005.

[7] M. Keshavarzi, A. Mohammadi, and A. Abdipour, "Characterization and compensation of DC offset on adaptive MIMO direct conversion transceivers," *IEICE Trans. Commun.*, vol. E94-B, no. 1, pp. 253–261, Jan. 2011.

[8] B. Lindoff and P. Malm, "BER performance analysis of a direct conversion receiver," *IEEE Trans. Commun.*, vol. 50, no. 5, pp. 856–865, May 2002.

[9] M. Krueger, R. Denk, and B. Yang, "Good and bad training sequences for zero IF sampling EDGE receivers," in *Proc. 2004 IEEE Int. Conf. on Acoust., Speech, and Signal Process.*, vol. 4, pp. 1033–1036.